



## Research Paper

## Synthesis and Application of Functionalized Carbon Nanotube Infused Polymer Membrane (fCNT/PSF/PVA) for Treatment of Phenol-Containing Wastewater

Michael O. Daramola <sup>1,\*</sup>, Olawumi O. Sadare <sup>1</sup>, Olugbenga O. Oluwasina <sup>2</sup>, Sunny E. Iyuke <sup>1</sup><sup>1</sup> School of Chemical and Metallurgical Engineering, Faculty of Engineering and the Built Environment, University of the Witwatersrand, Wits2050, Johannesburg, South Africa<sup>2</sup> School of Chemistry, Faculty of Science, Federal University of Technology, Akure, Nigeria

### Article info

Received 2018-11-25  
 Revised 2019-05-03  
 Accepted 2019-06-11  
 Available online 2019-06-11

### Keywords

Carbon nanotubes  
 Refinery wastewater  
 Phenol  
 Membrane  
 Polymer

### Highlights

- CNTs were functionalized to enhance dispersion and degree of hydrophilicity in PSF.
- PSF membrane was infused with functionalized CNTs and the membrane coated with PVA
- Effect of incorporation of fCNTs and PVA coating was studied during treatment of phenol-containing wastewater
- Incorporation of fCNTs and PVA coating improved the membrane flux and selectivity to phenol

### Abstract

In this study, polymer composite membranes comprising carbon nanotube (CNT), polysulfone (PSF) and polyvinyl alcohol (PVA) were synthesized via the phase inversion method and used to remove phenol from the phenol-containing wastewater. The fabricated membranes were reinforced with the functionalized carbon nanotubes (fCNTs) and coated with PVA to enhance their mechanical strength and anti-fouling property, respectively. Performance of the membranes was evaluated for the treatment of the synthetic phenol-containing wastewater using a dead-end filtration cell operated at different feed pressures in the range of 1-8 bar. The non-coated membrane with 5% fCNTs displayed the highest flux of  $70.21 \text{ L.m}^{-2}.\text{h}^{-1}$ , followed by the PVA coated membrane loaded with 5% fCNTs displaying flux of  $59.63 \text{ L.m}^{-2}.\text{h}^{-1}$ . The results showed that the non-coated PSF membrane loaded with 5% CNTs displayed the highest permeability of  $28.24 \text{ L.m}^{-2}.\text{h}^{-1}.\text{bar}^{-1}$  at transmembrane pressure (TMP) of 1 bar. Pure PSF with 0% loaded fCNTs showed the lowest permeability of  $0.68 \text{ L.m}^{-2}.\text{h}^{-1}.\text{bar}^{-1}$  at TMP of 1 bar. Analysis of the constituents of the wastewater using a pre-calibrated Gas chromatography-Mass chromatography (GC-MS) reveal that the membrane reinforced with fCNTs (1% CNT loading) and coated with PVA displayed the highest phenol rejection of 65%. It is noteworthy to mention that all the membranes showed 100% selectivity to the hydrocarbons (petrol and kerosene) contained in the wastewater. The results of this study could be a platform to develop cost-effective membrane materials for treatment of the refinery wastewater at low pressure for low energy consumption.

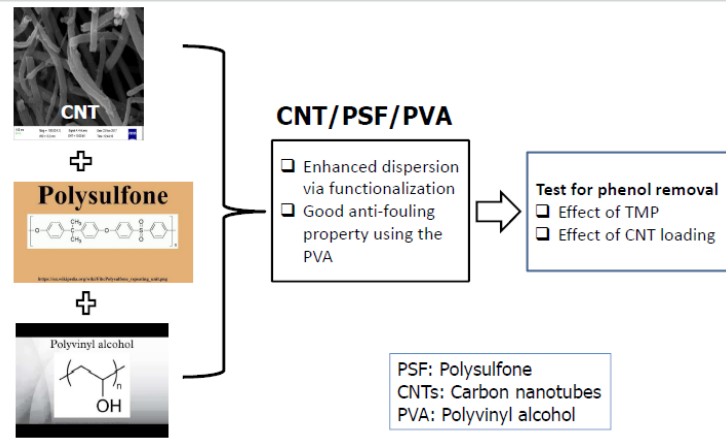
© 2019 MPRL. All rights reserved.

### 1. Introduction

Water is the central element of all vital social and economic processes. Thus, increasing in population and industrialization, as well as development of consumer society, harmful compounds (organic and inorganic chemicals) are generated in large quantities from industry throughout the world. The

problems derived from the toxicological effects of these compounds must be resolved for the benefits of entire society [1]. The problem is certainly complex and it is imperative that novel procedures are required to proffer lasting solutions to these problems. Several treatment technologies for

### Graphical abstract



\* Corresponding author at: Phone: +27117177536  
 E-mail address: Michael.Daramola@wits.ac.za (M.O. Daramola)

DOI: 10.22079/jmsr.2019.98343.1235

sewage, distillery effluents etc., which contain biodegradable organics, exist but a few technologies developed for treating toxic effluents containing xenobiotic compounds that are often non-biodegradable or only partially biodegradable. Biological treatment, though promises much in this regard, is handicapped by its slow oxidation characteristics and incomplete mineralization of toxic chemicals [2-4]. Application of nanotechnology has also improved the versatility of membrane filtration process for water treatment. For instance, nanofiltration (NF) and reverse osmosis (RO) are two common membrane filtration processes for toxic chemical removal from wastewater and have been successfully applied in removing biological oxygen demand (BOD)/ chemical oxygen demand (COD) from wastewater [5,6].

Nanofiltration provides numerous benefits over other types of membrane technology. It is cost effective; retains high multivalent anions salts; operates at low pressure; relatively cheap in terms of maintenance; retains high organic molecules; and environmentally friendly [7,8]. In membrane separation process, the liquid to be separated circulates with movement parallel to the filtering surface, thereby allowing adequate unrest to avoid fouling [9]. The separation requires a driving force called the transmembrane pressure (TMP). Transmembrane pressure is the pressure difference between the feed side and the permeate side of the membrane and the performance evaluators of a good membrane material are flux and rejection (selectivity). Furthermore, membrane fouling, which is the buildup of unwanted substances at the pores or on the surface of a membrane, still constitutes a major challenge encountered in membrane process [10,11]. Membrane fouling is indicated by a decline in the membrane flux and hence a loss in the performance of the membrane [10,11]. In some cases, membrane fouling could be minimized by modifying the surface of the membranes or embedding some nanoparticles such as carbon nanotubes, hydroxy sodalite etc. within the polymer matrix of the membranes [12-14]. The use of carbon nanotubes (CNTs) as fillers has received great attention by researchers in membrane technology due to their excellent properties, like excellent thermal, mechanical, and electrical properties. However, their tendency to form agglomerates due to van der Waal force makes their dispersion in polymer matrix challenging. Overcoming this shortcoming requires functionalization of the CNTs to achieve good interfacial interaction between the CNTs and the polymer, thereby enhancing the dispersion.

Polysulphone (PSF) membranes are the most common membranes used in ultrafiltration of wastewater due to its mechanical robustness and structural and chemical stability. Unfortunately, these membranes are mostly hydrophobic in nature and therefore highly susceptible to fouling. Many studies have been conducted to increase the hydrophilic properties of polysulphone/ polyethersulfone membranes [15]. Suitable modification of the membrane is probably the most sustainable approach to obtain fouling-resistant membranes. This would require the insertion of hydrophilic groups into a polymeric structure, so that the overall material becomes more hydrophilic and thus less prone to (organic) fouling. Poly vinyl alcohol (PVA), which is a water-soluble biodegradable polymer with different degrees of hydrolysis, is a promising candidate for this purpose due to its hydrophilicity and film forming characteristics. It is well known that membrane selectivity can be enhanced through modification of chemical structure of polymer membrane via cross-linking and grafting [12]. Furthermore, operating pressure and temperature have been reported to have significant effect on membrane flux [14, 16]. It is known that increasing the filtration pressure (transmembrane pressure) enhances the membrane flux but to the detriment of the membrane selectivity. Therefore, there is always a trade-off between the membrane selectivity and the membrane flux. Hence, an optimal point is always sought for economic viability of the membrane operation.

Against this background, synthesis and performance evaluation of CNT infused PSF membrane with enhanced anti-fouling property using functionalized CNTs and PVA have been reported. Therefore, in this current study, CNTs were functionalized and incorporated in the polysulfone membrane for wastewater treatment.

## 2. Experimental

### 2.1. Materials

CNTs (purchased from Sigma Aldrich, South Africa), Petrol, Kerosene (purchased from a gas station in Johannesburg) and phenol (99.99% purity purchased from Sigma Aldrich, South Africa) were used in the study. Nitrogen gas (99.99% purity, purchased from Merck South Africa) and Helium gas (technical grade, purchased from Afrox) were used as well. The deionized water used in the experiment was produced in-house.

### 2.2 Purification and functionalization of CNTs

Purification of the as-purchased CNTs (aCNTs) was carried out using the modified method of Uchechukwu et al. [17] to produce purified CNTs (pCNTs). CNTs were purified using 3:1 ratio of concentrated acetic acid and concentrated hydrochloric acid with CNTs-to-liquid ratio of 1:100. A reflux unit with operating conditions: stirring temperature, 80 °C; stirring time, 24 h; and stirring speed, 400 rpm; was used. The material obtained after the purification was then washed using deionized water to a neutral pH and dried in an oven at room temperature for 24 h and then at 50 °C for another 24 h to remove the moisture to attain a constant weight.

For the functionalization of the pCNTs to give functionalized CNTs (fCNTs), all the operating conditions employed in the purification were maintained except that the chemicals used in the functionalization were 500 mL of 0.5 M H<sub>2</sub>SO<sub>4</sub> and 10 g of KMnO<sub>4</sub>. After the completion of the functionalization, the functionalized material was washed with concentrated HCl to remove MnO<sub>2</sub>. Then the acid-washed functionalized CNTs were washed with deionized water to a neutral pH and dried in an oven, first at room temperature for 24 h and then at 50 °C for another 24 h to a constant weight as described by Slobodian et al. [18]. The functionalized CNTs were characterized using XRD for crystallinity and phase identification; Raman spectroscopy for purity; FTIR for surface chemistry; and TEM for morphology.

For the fabrication of the membrane using the fCNTs, the phase inversion method as described in the literature was adopted [13]. A device known as 'Dr Blade' was used to cast the homogenized casting solution on a glass. About 10 g of polysulfone (PSF) was added to 50 mL of dimethylformamide and 0.5 g of CNTs to form the casting solution. The mixture was sonicated for 10 min and stirred on a magnetic stirrer for 24 h at 400 rpm. Then the homogenized solution was sonicated for 10 min to remove air bubble therein and then cast on a glass plate using the casting blade. Firstly, the cast material was left for 10 s to allow evaporation of the solvent and thereafter immersed in deionized water for 24 h and dried at 125 °C for 15 min. Different samples of membranes namely: PSF coated with PVA (PSF/PVA), PSF not coated with PVA (PSF/nPVA), fCNT loaded PSF and coated with PVA (wt.% fCNT/PSF/PVA); fCNT loaded PSF but not coated with PVA (wt.% fCNT/PSF/nPVA), PSF coated with PVA but not loaded with fCNTs (0wt.% fCNT/PSF/PVA) were fabricated, characterized and evaluated in this study.

### 2.2. Performance evaluation of the membranes

The original flux of the membranes was evaluated by conducting pure water permeation through the membranes using the deionized water and a filtration cell operated at dead-end mode at pressures of 2 bar to 8 bar. Consequently, the pure water flux and the pure water permeability of the membranes were determined. Synthetic refinery wastewater containing phenol (4 g/L=0.05 M), kerosene (5 g/L) and gasoline (5 g/L) was prepared and used to evaluate the phenol removal efficiency of the membrane. The synthetic refinery wastewater was prepared by mixing 4.7 g/L of Phenol (0.05M), 5 g/L of unleaded petrol and 5 g/L of Kerosene and stirred continuously at 750 rpm for 3 h to obtain a homogeneous solution. The treatment of the wastewater was carried out on a filtration cell operated at a dead-end mode at pressures ranging from 2 to 8 bar using the same membrane employed for pure water permeation. The mixture was stirred continuously during the separation to maintain homogeneity of the solution. To induce the desired TMP on the membrane in the cell, N<sub>2</sub> gas was supplied through the inlet of the cell to provide the desired pressure (see Figure 1). Before separation commenced, the membrane was equilibrated for 1 h to open the pores and give room for easy passage of the water (permeate) through the membrane. The filtration was carried out at a feed pressure ranged from 1 bar to 8 bar and the filtration time was 1 h at each pressure change using a membrane area of 3.42 x 10<sup>-3</sup> m<sup>2</sup>. Figure 1 shows the description of the set-up used in the study for the wastewater separation. The permeate was collected in a graduated cylinder and recorded.

The analysis of the feed, retentate and permeate was done using a pre-calibrated Gas chromatography-Mass chromatography (GC-MS) (QP2010 Ultra, Shimadzu). The mobile phase was helium gas and at column temperature of 50 °C; injection temperature of 180 °C and pressure of 1 bar. About 1 μL of the sample was injected into the GC column and the analysis was carried out at a set time of 25 minutes. Pure water flux from the membrane and during the separation, permeance (permeability) and rejection (selectivity) of the membrane were obtained using Equation (1), Equation (2), and Equation (3), respectively:

$$F = \frac{V}{A} \quad (1)$$

$$P = \frac{F}{\text{TMP}} \quad (2)$$

$$R = \frac{C_F - C_P}{C_F} \times 100 \quad (3)$$

where  $V$  is volumetric flowrate ( $\text{L.h}^{-1}$ ),  $A$  is the effective area of the membrane ( $\text{m}^2$ ),  $P$  is the permeability ( $\text{L.m}^{-2}\text{h}^{-1}\text{bar}^{-1}$ ), TMP is transmembrane pressure (bar); and  $R$  is the oil rejection (selectivity) of the membrane expressed in percentage.  $C_F$  is oil (phenol) concentration in the feed to the dead-end mode unit ( $\text{mg/l}$ ) and  $C_P$  is the oil (phenol) concentration in the permeate.

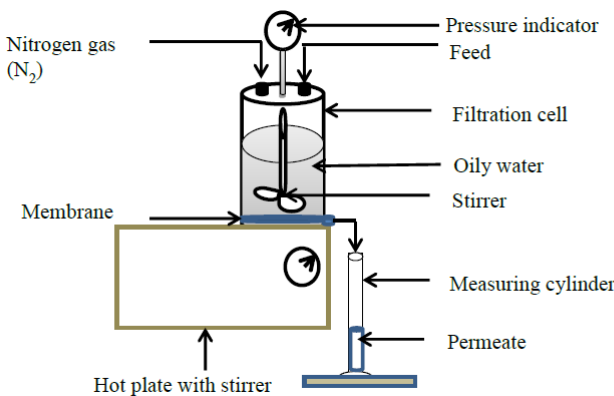


**Fig. 1.** Schematic of the filtration set-up operated at dead-end mode for the oil-water separation.

### 2.3. Physico-chemical characterization of CNTs and FCNTs

X-ray diffraction spectroscopy (XRD), Scanning electron microscopy (SEM), Transmission electron microscopy (TEM), Raman spectroscopy and Fourier transmission infrared (FTIR) spectroscopy were used to check the crystallinity and phases, surface morphology, purity and surface chemistry, respectively, of the CNTs. X-ray diffractometer (Bruker D2 X-ray diffractometer) was used to check the crystallinity and phase composition of the aCNTs, the pCNTs and the fCNTs. The phase composition was checked against the PLU2018-pdf-4-2018RDB database using EVA software. The surface morphology of aCNTs, pCNTs and fCNTs were checked using a Field Electronic Scanning Electron Microscope (FESEM) (CARL ZEISS sigma) and by Transmission Electron Microscopy (TEM) (JEOL 100S Electron Microscope, Tokyo, Japan). The properties of the CNTs observed under TEM were also confirmed by Raman spectroscopy (J-Y T64000 micro-Raman spectrometer, Horiba Jobin-Yvon, Ltd., Stanmore, UK). FTIR analyzer, at a wave number range of  $500 \text{ cm}^{-1}$  to  $4000 \text{ cm}^{-1}$  was used to check the attachment of functional groups on the aCNTs, fCNTs and pCNTs.

## 3. Results and discussion

### 3.1. Physico-chemical characterization of CNTs (aCNTs, pCNTs and fCNTs)

The XRD patterns of the aCNTs, the pCNTs and the fCNTs are depicted in **Figure 2**. The XRD patterns indicate the preservation of the crystalline and morphology nature of CNTs after the purification and functionalization. Although, it was observed that there was an increase in the intensity of diffraction peaks at (002) from aCNTs to fCNTs, which could be attributed to the loss of the CNT "floss" after the acid treatment [19]. The XRD patterns further present the characteristic CNTs diffraction peak at about  $26.5^\circ$  [20], indicating that CNTs structure was not destroyed by the acid combination used for the purification, but carbonaceous materials must have been removed leading to increase in the crystallinity of the CNTs.

The TEM images of the aCNTs, the pCNTs and the fCNTs are depicted in **Figure 3**. An arrow with label 'b' on the image shows the multi-walled

characteristics of the CNTs, and an arrow with label 'a' shows the presence of significant amount of the amorphous carbon. There was improvement in the purity of the CNTs as shown in the TEM image of pCNTs, because there was a reduction in the amorphous carbon (as depicted by arrow 'b') by the acid purification method. Also the TEM image of pCNTs indicates that side wall characteristics of the CNTs were preserved (label 'a'). From the TEM image of fCNTs, it could be observed that the oxidation process also reduced the amount of the amorphous carbon (see label 'b') with preservation of the structure of the CNTs (see label 'a'). These results showcase the potential of the purification and functionalization method employed in this study in purifying and functionalizing CNTs without losing the crystallinity and changing the morphology of the CNTs. In addition, results of this study are in agreement with literature [21].

The Raman spectra of aCNTs, pCNTs and fCNTs are depicted in **Figure 4**. The two peaks at approximately  $1325 \text{ cm}^{-1}$  (as D-band) and at  $1530 \text{ cm}^{-1}$  as (G-band) are indicated on the Raman spectra of the aCNTs, pCNTs and fCNTs (see **Figure 4**). The  $I_D/I_G$  intensity ratio measures the defects, purity and modification [22]. The  $I_D/I_G$  intensity ratio of aCNTs was 0.84, and it decreased slightly after purification due to removal of the impurities such as amorphous carbon and unused catalyst. The insignificant decrease indicates non-destructive nature of the chemical used during the purification. The increase in the ( $I_D/I_G$ ) of the fCNTs to 0.85 from 0.84 recorded for the pCNTs is an indication of introduction of functional groups to the carbon surface. The inference is that the acids used for the purification did not affect the structural composition of the CNTs and this agrees with the result of Yadianti et al. [23]. The FTIR spectra of the CNTs as shown in **Figure 5** are unexpected spectra. All the CNTs (aCNTs, pCNTs and fCNTs) are devoid of any identified CNT functional groups at about  $2000 \text{ cm}^{-1}$ ,  $2250 \text{ cm}^{-1}$  and  $2500 \text{ cm}^{-1}$ . Similar observation has been reported by Aviles et al. [24]. In their study, Aviles and co-workers observed unidentifiable functional groups in their FTIR spectra. However, some functional groups were introduced after purification and functionalization. The intensities of groups introduced on the surface of pCNTs and fCNTs are much weaker due to the low concentration of groups. The purified carbon nanotube (pCNTs) had some additional functional groups at about  $2850 \text{ cm}^{-1}$  and  $2980 \text{ cm}^{-1}$ , attributable to asymmetric and symmetric  $\text{CH}_2$  stretching. Also, there appeared (though not too broad) functional group assigned to OH at about  $3500 \text{ cm}^{-1}$ . The fCNTs showed same functional groups as that of the pCNTs with an increased intensity at  $3500 \text{ cm}^{-1}$ , attributable to the functionalization of the CNTs that increased the concentration of the OH functional group on fCNTs. The results of the Raman analysis also indicate that the functional group induced onto the pCNTs after functionalization was weaker, (because the ( $I_D/I_G$ ) was from 0.84 to 0.85, indicating introduction of functional groups to the surface of the CNTs). It is noteworthy to mention that the purification method did not destroy the side wall of the CNTs where the functional group could be attached. However, the scientific reason behind the introduction of the unidentifiable functional groups on the carbon nanotube and the introduction of functional groups on the pCNTs after HCl and acetic acid treatment are yet unknown, therefore more research efforts are needed to unravel this uncertainty.

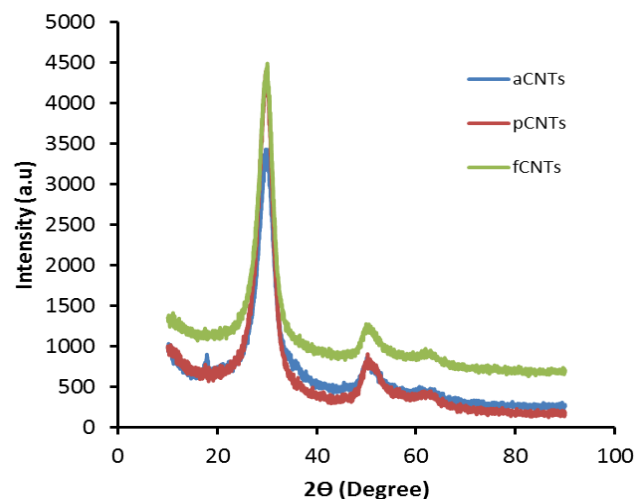


**Fig. 2.** XRD patterns of aCNTs, pCNTs in 3:1 concentrated acetic acid, fCNTs with 0.5 M  $\text{H}_2\text{SO}_4$  and 10 g  $\text{KMnO}_4$ .

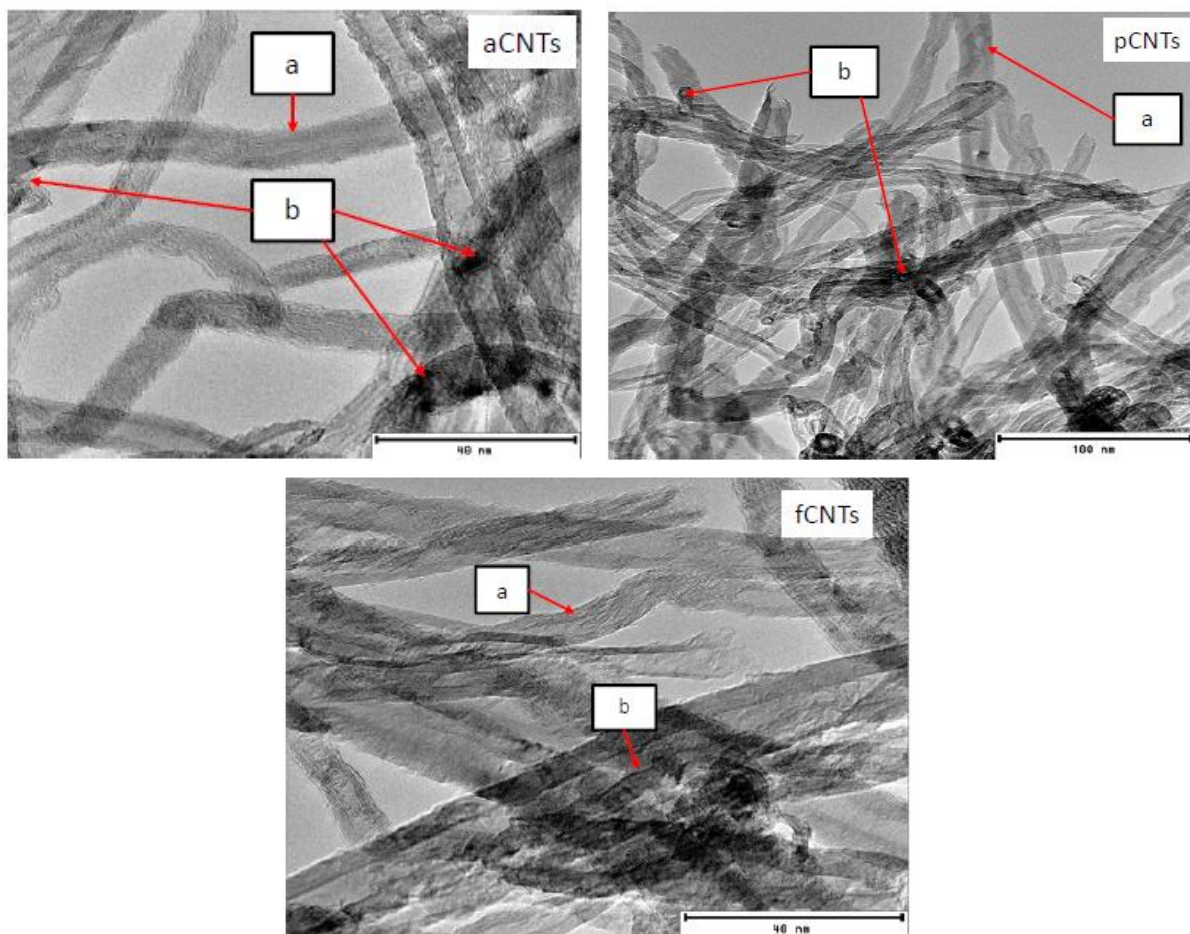


**Fig. 3.** TEM images of aCNTs, pCNTs and fCNTs.

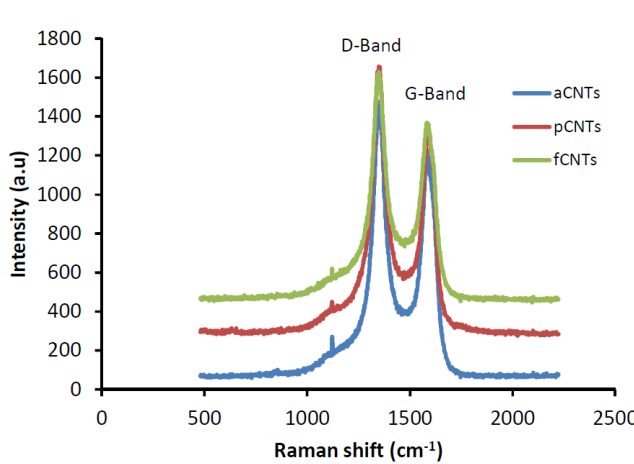


**Fig. 4.** The Raman shift for the aCNTs, fCNTs and the pCNTs.

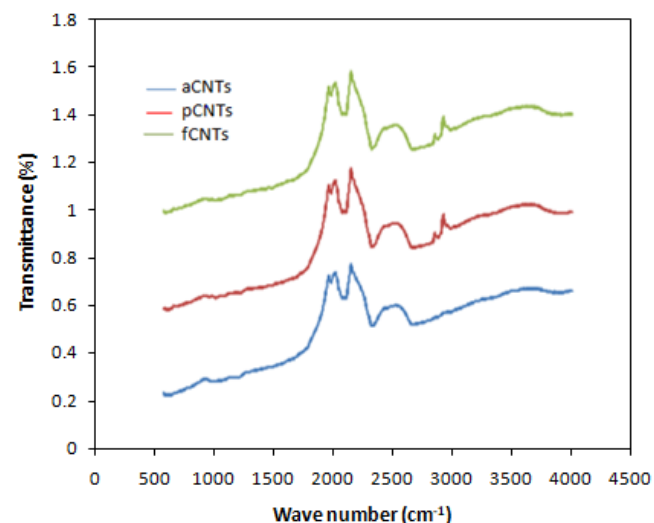


**Fig. 5.** FTIR spectra of the aCNTs, pCNTs and fCNTs

### 3.2. Physico-chemical characterization of membrane

The characterized fCNTs were incorporated in the polymer to make the membranes described in Section 2.2. The sample of the 1 wt.% fCNTs loaded PSF/PVA membranes and their SEM images are depicted in Figure 6. Average thickness of the membrane obtained from a digital micrometer gauge

was 0.08 mm. The SEM image of the surface view shows no clearly visible pores (see Figure 6(b)), attributable to the hydrophilic PVA layer that covered the surface of the membrane [12]. However, the SEM image of the cross-sectional view of the membrane confirms the presence of the CNTs (see Figure 6(b)).

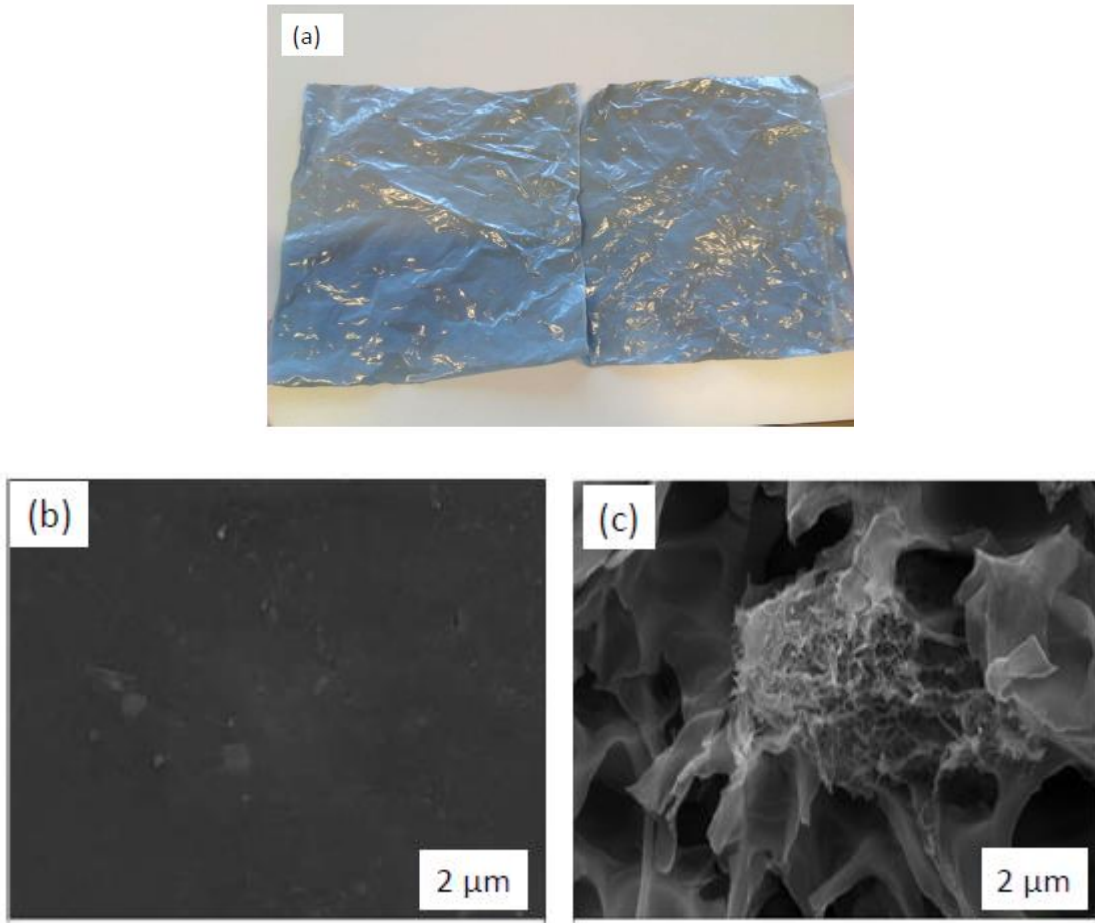


**Fig. 6.** Fabricated membranes. (a) samples of 1 wt.% fCNT/PSF/PVA membranes; (b) SEM image of the surface view of 1 wt.% fCNT/PSF/PVA; (c) SEM image of the cross-sectional view of 1 wt.% fCNT/PSF/PVA.

The contact angle of the fCNT loaded PSF and coated with PVA (wt.% fCNT/PSF/PVA) membrane was  $71^\circ \pm 6$  and that of the PSF not coated with PVA (PSF/nPVA) membrane was  $81^\circ \pm 3.4$ , indicating that hydrophilicity of the (PSF/nPVA) membrane was enhanced after embedding it with fCNTs and coating it with PVA [25,26].

### 3.3. Performance evaluation of the membranes

Figure 7 shows the permeate flux of deionized water and that of the phenol-containing wastewater through the membrane at pressures of 2, 3, 5 and 8 bar. In both cases, results show that the permeate flux increased with increase in pressure. Increasing the pressure enhanced the driving force for permeation, resulting in the high permeation flux [21]. In addition, the water flux of pure polysulfone membrane coated with polyvinyl alcohol is higher than that of the pure PSF membrane with no coating. This is an indication that PVA enhanced the permeability of the membrane due to the hydrophilic nature of the PVA. However, when fCNTs were incorporated into the membranes (PSF), an increase in flux was observed because of the presence of the hydrophilic fCNTs in the membrane structure [27]. These fCNTs, with probable good dispersion in the membrane, improved the hydrophilicity and increased the water flux through the membrane. There was noticeable decrease in the permeate flux of fCNTs-incorporated PSF membrane with PVA coating when compared to that of fCNTs-incorporated PSF membrane without PVA coating. This may be as a result of the PVA layer on the surface of the fCNTs-incorporated PSF membrane with PVA coating membrane which hinders the permeation of water. Also, at increased concentration of fCNTs, the permeate flux increased. This could be because of increase in pore size which resulted from an increase in CNTs concentration [12]. The 5% fCNTs loaded PSF without PVA coating displayed the highest permeate flux of  $70.21 \text{ L.m}^{-2} \cdot \text{h}^{-1}$ , followed by the 5% fCNTs loaded PSF with PVA coating with a flux of  $59.63 \text{ L.m}^{-2} \cdot \text{h}^{-1}$ .

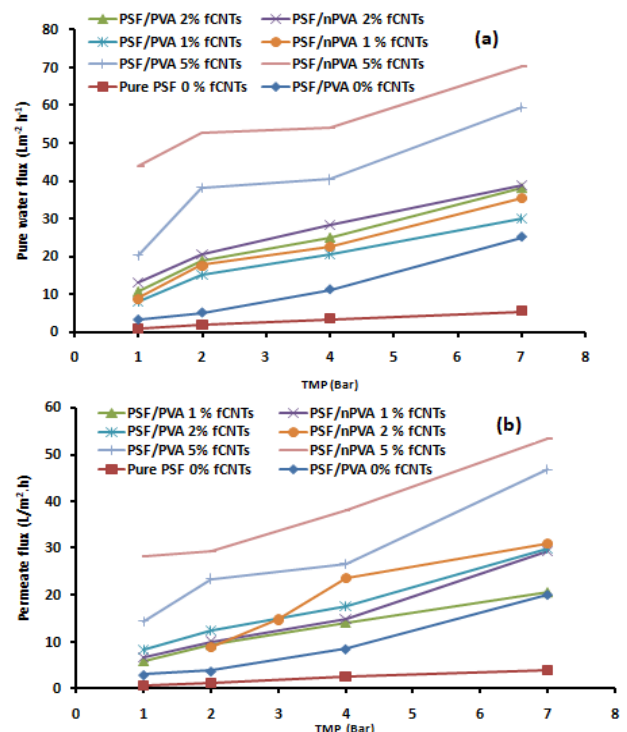


**Fig. 7.** Membrane flux as a function of pressure. (a) Pure water permeation; (b) Permeation of phenol-containing wastewater during filtration.

Regarding the effect of increase in the feed pressure, the membrane flux increased at increasing the feed pressure, attributable to enhance the driving force (TMP) as the feed pressure increased. The increase in flux at higher feed pressure could be attributed also to the rapid permeation of water droplets through the membrane pores and denser surface of the PVA under the higher TMP as suggested by Jin et al. [28]. It should be noted that these membranes showed a decline in flux during the treatment of phenol-containing wastewater, indicating fouling and pronounced competitive sorption between the components and water.

**Table 1** shows the permeability of pure water with reference to TMP. The result shows that the permeability decreased with an increase in TMP, but increased with an increase in fCNT loading. For the treatment of phenol-containing wastewater, results in **Table 1** show also an increase in permeability at increasing TMP and the permeability increased with an increase in fCNTs loading as well, although not with much visible difference, except at 5 wt.% fCNT loading. This could be because the structure of the PSF layer has been altered by the increasing addition of fCNTs [28]. The incorporation of CNTs in the membrane influences the permeability of the membrane as well as the pure water flux, confirming that addition of the fCNTs improved the performance of the membrane [13]. However, the decrease in the permeability observed during the treatment of phenol-containing wastewater when compared to the performance during the pure water permeation from pure water could be because of the presence of the oxygen-containing functional groups on the fCNTs [13]. In addition, it could be attributed to fouling of the membrane surface by deposition of other components in the wastewater.

#### 3.4. Effect Concentrations of fCNTsand pressures on the Rejection Capacity of the Membranes for Phenol removal

Effect of the incorporation of fCNTs in the PSF and the coating with PVA on the phenol rejection during the treatment of phenol-containing wastewater at TMP of 2 bar is depicted in **Figure 8**. **Figure 9** shows phenol rejection of PSF membrane loaded with 1% fCNTs and coated with PVA as a function of TMP and **Figure 10** compares the performance of the PSF membrane loaded with 1% fCNTs and coated with PVA toward other component in the wastewater. **Figure 8** shows that the phenol rejection decreased as fCNTs loading increased from 1% to 5% for both membranes with and without PVA. Membrane with 1% fCNTs loading and with PVA displayed the highest phenol rejection of 64.9% attributable to PVA layer that enhanced the selectivity. At increasing TMP, **Figure 8** shows a decrease in the phenol rejection. This indicates that at high TMP, there was increase in the concentration of phenol in the permeate. This could be attributed to increase in the transmembrane pressure, which rose above the capillary pressure of the membrane that prevents the phenol from permeating, thereby resulting into forceful permeation of the phenol through the pores. The membrane displayed almost 100% selectivity to kerosene and unleaded gasoline (see **Figure 10**). As there were no traces of these components in the permeate as indicated from the pre-calibrated GC-MS employed in the analysis. Although non-detection of these compounds could be because of the low detection limit of the GC-MS, however the results obtained using the instrument corroborate the observation. However, 65% membrane rejection capacity was calculated for phenol with 0.1CNTs/PSF coated with PVA with 1% fCNTs loading. In addition, this could be as a result of chains of hydrocarbon present in kerosene and petrol. In addition it is speculated that the molecular size of petrol and kerosene is higher than the diameter of the membrane, preventing them from being transmitted through the membranes, although more investigation might be needed on this.

**Table 1**

Pure water permeation as a function of transmembrane pressure (TMP).

TMP (Bar)		Permeability of pure water for membrane samples (L/m <sup>2</sup> .h.bar)							
		Pure PSF (0% fCNTs)	PSF/PVA (0% CNTs)	PSF/PVA 1% fCNTs	PSF/nPVA 1% fCNTs	PSF/PVA 2% fCNTs	PSF/nPVA 2% fCNTs	PSF/PVA 5% fCNTs	PSF/nPVA 5% fCNTs
1		0.899	3.199	7.959	8.859	10.669	13.095	20.265	43.941
2		0.904	2.533	7.527	8.798	9.412	10.326	19.189	26.307
4		0.864	2.809	5.137	5.663	6.226	7.066	10.121	13.519
7		0.779	3.584	4.280	5.065	5.428	5.562	8.518	10.030
TMP (Bar)		Permeability of refinery waste water (L/m <sup>2</sup> .h.bar)							
1		0.68	2.99	5.85	6.72	8.30	8.83	14.24	28.24
2		0.90	2.53	4.68	5.04	6.26	7.37	11.69	14.64
4		0.86	2.80	3.51	3.70	4.40	5.89	6.45	9.51
7		0.78	3.58	2.93	4.18	4.28	4.44	6.68	7.60

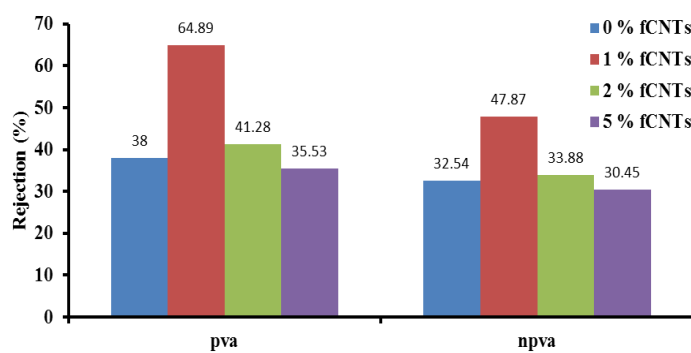


**Fig. 8.** Phenol rejection of membranes at different fCNTs loading. Experimental conditions: Pressure 2 bar; Concentration of Phenol 0.05 M; Time 3 h.

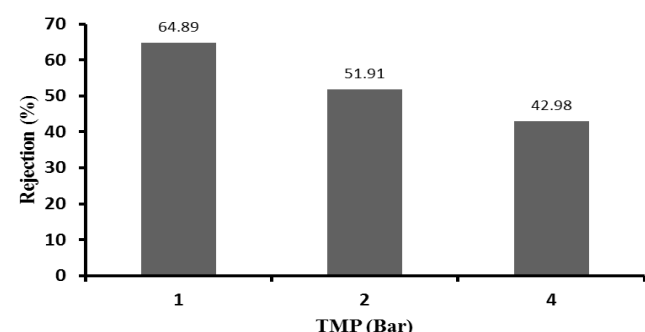


**Fig. 9.** Phenol rejection of PSF membrane loaded with 1% fCNTs and coated with PVA as a function of TMP. Experimental conditions: Phenol concentration 0.05 M; Time 3 h.

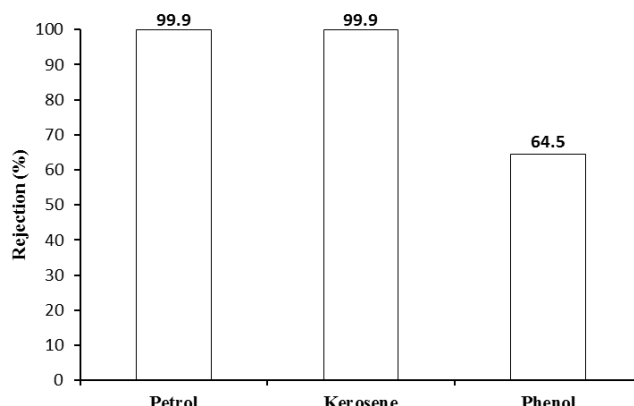


**Fig. 10.** Phenol rejection of PSF membrane loaded with 1% fCNTs and coated with PVA compared to other hydrocarbons in the wastewater.

#### 4. Conclusions

Results from this study have shown that the membrane reinforced with the functionalized CNT (at low loading) and coated with PVA displayed the highest phenol rejection while PSF loaded with 5wt.% fCNTs but with no PVA layer displayed the lowest phenol rejection. Also, the results reveal a decrease in rejection with increase in pressure and increase in concentration of the CNTs in the polymer membrane. It is noteworthy to mention that the PSF membrane loaded with 1wt.% fCNTs and coated with PVA displayed rejection of about 100% (99.9%) for both kerosene and petrol with a rejection of 65% for phenol at TMP of 1 bar. This indicates that embedding CNTs in PSF enhanced its rejection rate and coating it with PVA improved the surface properties of the membranes, as well. Analysis of the permeate from the membrane shows the hydrocarbon (petrol and kerosene) rejection of 100% and the phenol rejection of 65%. In addition, results of this study indicate that fabricating the membrane using very small amount of fCNTs and using the membrane at a much reduced pressure could make the membrane application cost effective and energy efficient for the treatment of the refinery wastewater, for the treatment of phenol-containing wastewater in particular.

#### Conflicts of interest

Authors declare no conflict of interest.

#### References

- [1] L.D. Naidu, S. Saravanan, M. Goel, S. Periasamy, P. Stroeve, A novel technique for detoxification of phenol from wastewater: Nanoparticle Assisted Nano Filtration (NANF), *J. Environ. Health Sci. Eng.* 14 (2016) 1-12.
- [2] X. Jin, E. Li, S. Lu, Z. Qiu, Q. Sui, Coking wastewater treatment for industrial reuse purpose: Combining biological processes with ultrafiltration, nanofiltration and reverse osmosis, *J. Environ. Sci.* 25 (2013) 1565–1574.
- [3] H. Kamani, S. Nasseri, M. Khoobi, R. Nabizadeh Nodehi, A.H. Mahvi, Sonocatalytic degradation of humic acid by N-doped TiO<sub>2</sub> nano-particle in aqueous solution, *J. Environ. Health Sci. Eng.*, 14 (2016) 3.
- [4] A. Naghizadeh, S. Nasseri, A.H. Mahvi, R. Nabizadeh, R.R. Kalantary, A. Rashidi, Continuous adsorption of natural organic matters in a column packed with carbon nanotubes, *J. Environ. Health Sci. Eng.* 11 (2013) 14.
- [5] E. Sahar, I. David, Y. Gelman, H. Chikurel, A. Aharoni, R. Messalem, A. Brenner, The use of RO to remove emerging micropollutants following CAS/UF or MBR treatment of municipal wastewater, *Desalination* 273 (2011) 142–147.
- [6] K. Chon, H. KyongShon, J. Cho, Membrane bioreactor and nanofiltration hybrid system for reclamation of municipal wastewater: Removal of nutrients, organic matter and micropollutants, *Biores. Technol.* 122 (2012) 181–188.
- [7] N. Hilal, H. Al-Zoubi, N.A. Darwish, A.W. Mohamma, M. Abu Arabi, A comprehensive review of nanofiltration membranes: Treatment, pretreatment, modelling, and atomic force microscopy, *Desalination* 170 3 (2004) 281–308.
- [8] H. Al-Zoubi, A. Rieger, P. Steinberger, W. Pelz, R. Haseneder, G. Härtel, Nanofiltration of acid mine drainage, *Desalin. Water Treat.* 21 (2010) 148–161.
- [9] C.A. Paraskeva, V.G. Papadakis, E. Tsarouchi, D.G. Kanelloupolou, P.G. Koutsoukos, membrane processing for olive mill wastewater fractionation, *Desalination*, 213 (2007) 218–229.
- [10] T.F. Speth, R.S. Summers, A.M. Gusses, Nanofiltration foulants from a treated surface water, *Environ. Sci. Technol.*, 32 (1998) 3612–3617.
- [11] J.R.V. Flora, Stochastic approach to modeling surface fouling of ultrafiltration membranes, *J. Membr. Sci.* 76 (1993) 85–88.
- [12] S. Maphutha, K. Moothi, M. Meyyappan, S.E. Iyuke, A carbon nanotube-infused polysulfone membrane with polyvinyl alcohol layer for treating oil-containing waste water, *Sci. Rep.* 3 (2013) 1509.
- [13] M.O. Daramola, P. Hlanyane, O.O. Sadare, O.O. Oluwasina, S.E. Iyuke, Performance of carbon nanotube/polysulfone (CNT/PSF) composite membranes during oil–water mixture separation: Effect of CNT dispersion method, *Membranes* 7 (2017) 14.
- [14] M.O. Daramola, B. Silinda, S. Masondo, O.O. Oluwasina, Polyethersulphonate-sodalite (PES-SOD) mixed-matrix membrane: Prospects for acid mine drainage (AMD) treatment, *J. S. Afr. Inst. Min. Met.* 115 (2015) 1221–1228.
- [15] H.L. Richards, P.G.L. Baker, E. Iwuoha, Metal nanoparticle modified polysulfone membranes for use in wastewater treatment: A critical review, *J. Surf. Eng. Mater. Adv. Technol.* 2 (2012) 183–193.
- [16] H. Al-Zoubi, A. Rieger, P. Steinberger, W. Pelz, R. Haseneder, G. Härtel, Optimization study for treatment of acid mine drainage using membrane technology, *Sep. Sci. Technol.* 45 (2010) 2004–2016.
- [17] C.W. Uchechukwu, S. Naga, S. Chalamalasetty, Z. Dong, M. Meyyappan, S.E. Iyuke, Dimensional analysis of acid etching effects on vertically grown carbon nanofibers using atomic force microscopy, *Nanomater. Nanotechnol.* 3 (2013) 1–8.
- [18] P. Slobodian, P. Riha, R. Olejnik, U. Cvelbar, P. Saha, Enhancing effect of KMnO<sub>4</sub> oxidation of carbon nanotubes network embedded in elastic polyurethane on overall electro-mechanical properties of composite, *Compos. Sci. Technol.* 81 (2013) 54–60.
- [19] N.A. Buang, F. Fadil, Z. A. Majid, S. Shahir, Characteristic of mild acid functionalized multiwalled carbon nanotubes towards high dispersion with low structural defects, *Digest J. Nanomat. Biostruct.* 7 (2012) 33–39.
- [20] F. Taleshi, A.A. Hosseini, Synthesis of uniform MgO/CNT nanorods by precipitation method, *J. Nanostruct. Chem.* 3 (2012) 4.
- [21] L. Stobinski, B. Lesiak, L. Köver, J. Tóth, S. Biniak, G. Trykowski, J. Judek, Multiwall carbon nanotubes purification and oxidation by nitric acid studied by the FTIR and electron spectroscopy methods, *J. Alloys Compound.* 501 (2010) 77–84.
- [22] O. Aberefa, K. Bedasie, S. Madhi, M.O. Daramola, S.E. Iyuke, Production of carbon nanotube yarn from swirled floating catalyst chemical vapour deposition: a preliminary study, *Adv. Nat. Sci. Nanosci. Nanotechnol.* 9 (2018) 035009.
- [23] R. Yudianti, R. Onggo, H. Sudirman, Y. Saito, T. Iwata, J.I. Azuma, Analysis of functional group sited on multi-wall carbon nanotube surface. *The Open Mat. Sci. J.* 5 (2011) 242–247.
- [24] F. Aviles, J.V. Cauch-Rodriguez, L. Moo-Tah, A. May-Pat, R. Vargas-Coronado, Evaluation of mild acid oxidation treatments for MWCNT functionalization, *Carbon* 47 (2009) 2970–2975.
- [25] R.S. Hebbal, A.M. Isloor, A.F. Ismail, S.J. Shilton, A. Obaid, H.K. Fun, Probing the morphology and antiorganic fouling behaviour of a polyetherimide membrane modified with hydrophilic organic acids as additives, *New J. Chem.* 39 (2015) 6141–6150.
- [26] K. Balakrishna Prabhu, M.B. Saidutta, Arun M. Isloor, R. Hebbal, Improvement in performance of polysulfone membranes through the incorporation of chitosan-(3-phenyl-1h-pyrazole-4-carbaldehyde), *Cogent Eng.* 4 (2017) 1403005.
- [27] S. Khoshrou, M.R. Moghboli, E. Ghasemi, Polysulfone/carbon nanotubes asymmetric nanocomposite membranes: Effect of nanotubes surface modification on morphology and water permeability, *Iranian J. Chem. Eng.* 12 (2015) 69.
- [28] X.W. Jin, E.C. Li, S.G. Lu, Z.F. Qiu, Q. Sui, Coking wastewater treatment for industrial reuse purpose: combining biological processes with ultrafiltration, nanofiltration and reverse osmosis, *J. Environ. Sci.* 25 (2013) 1565–1574.